BURNING BEHAVIOUR OF ENERGETIC IONIC LIQUIDS INVESTIGATED WITH 4-AMINO-1-METHYL-1,2,4-TRIAZOLIUMNITRAT

Volker Weiser, Uwe Schaller,

Wolfgang Becker, Diana Bieroth, Jürgen Hürttlen, Sebastian Knapp, André Lity, Evelin Roth

Fraunhofer Institut für Chemische Technologie (ICT)

Joseph-von-Fraunhofer-Straße 7, 76327 Pfinztal, Germany

volker.weiser@ict.fraunhofer.de

Abstract

4-Amino-1-methyl-1,2,4-triazoliumnitrat (C1 N or AMTN) is a typical representative of energetic ionic liquids, which can be produced in technical scale. It was used as a model substance to investigate the decomposition and high-pressure burning behavior under inert test conditions. Thermoanalytical studies indicate a complex exothermic decomposition process with at least four overlapping main reaction steps from 480 K to 540 K. After complete gasification at 540 K N_2O, CO, H_2O, HCN and NH_3 were identified as decomposition products by FTIR-analysis. The burning behavior was investigated in a window bomb as a function of pressure and initial temperature. The pure C1 N could only be ignited above 10 MPa. Then it burns with a linear progression rate between 6 and 9 mm/s without significant dependency on pressure and on initial temperature. A hot solid or gelatinous reaction zone of about 1 mm thickness was detected at the burning surface of the EIL. In NIR-emission spectra from the flame zone, strong bands related to primary and secondary amines and amides were detected. The visual and spectral investigations reveal a qualitative explanation of the pressure independence.

Introduction

By definition, salts being liquid (ILs) below 100°C are defined as ionic liquids [1]. They are in the focus of recent research and find application in more and more fields of life. The applications range from novel reaction media [2], as electrolytes in batteries [3], solar cells [4], gas storing media [5], lubricants [6] and heat transfer

fluids [7], to mention only a small excerpt of the investigated and in-use applications. The research on ILs already began in 1888 with ethanolammonium nitrate (mp 52-54 °C), an energetic protic IL synthesized and characterized by Gabriel [8] and ethylammonium nitrate (mp 13-14 °C; Paul Walden 1914 [9]). However, the new class of ionic liquids only became subject of interest in the late 1990s when the publications on ILs started growing exponentially. Using nitrogen-rich cations and oxygen-rich anions, it is possible to obtain so-called energetic ionic liquids. Shreeve et al. [10] already investigated a series of new energetic ionic liquids (EILs) but there is still a big undiscovered field due to the great number of possible combinations of energetic anions and cations. The general principle behind EILs is shown in Figure 1.

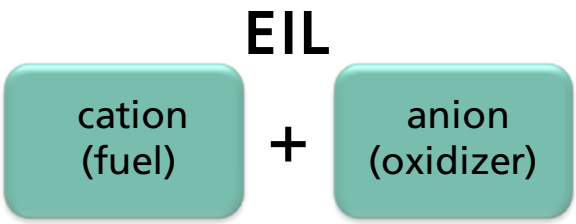

Figure 1 General principle of Energetic Ionic Liquids (EILs)

Potential applications are energetic plasticizers or liquid rocket and gun propellants. As an example of an energetic ionic liquid, we investigated 4-Amino-1-methyl-1,2,4-triazole (C1 N or AMTN), which was first mentioned in literature 2002 by Greg W. Drake et al. [11].

C1 N offers a wide operational temperature range from the glass transition temperature of -54 °C to the decomposition temperature above 200 °C. Due to its ionic nature the density of the EIL is quite high 1.4 g/cm^3 compared to traditional energetic monopropellants like hydrazine or nitromethane. The mechanical sensitivity of C1 N towards friction and impact is low (20 Nm and >360 N) as shown in Table 1.

Table 1: Physical data of C1 N, mechanical sensitivity data and chemical structure of C1 N

state		liquid
T_g	[°C]	-54
T_{dec} (TGA)	[°C]	249
density	[g/cm^3]	1.4
standard enthalpy of formation	[kJ/mol]	+33
impact sensitivity	[Nm]	20
friction sensitivity	[N]	>360

C1 N

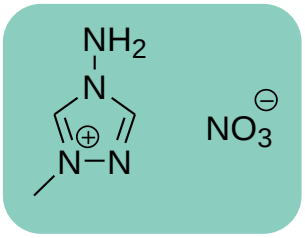

In ionic liquids, even small amounts of impurities (water, solvents or other ions) change the physiochemical properties significantly. Different theoretical enthalpies of formation of C1 N were published [12] (Table 2). The difference between highest and lowest value of the enthalpy of formation is 184 kJ/mol.

Table 2: Published theoretical enthalpy of formation values for C1 N

	Gumz	Lloyd-Davenport	Dulong-Berthelot	Garvin	Diallo	Shreeve	own value (exp.)
$\Delta_f H_m^\circ$ (C1 N) [kJ/mol]	-114	-87	+70	-38	+25	+57	33 ± 4

The only published value for C1 N based on an experimentally determined heat of combustion ($\Delta_{comb}H_m^\circ$ = -187.36 kJ/mol [13]) was carried out using C1 N synthesized via the silver route. It should be noted that for this value, no silver residue content is published and the reported measured density of 1.55 g/cm^3 is extremely high. The reported value of +33 kJ/mol in this paper was calculated form experimental heat of combustion measurements taking into account the formation of nitric acid.

Not taking into account the formation of nitric acid would lead to a higher enthalpy of formation and could explain the high measured combustion temperatures (see below).

The theoretical values and calculated performance of C1 N are shown in Table 3.

Table 3: Theoretical values and calculated performance of C1 N.

oxygen balance	[%]	-64.6
nitrogen content	[%]	43.5
heat of explosion	[J/g]	3468
specific energy	[J/g]	975
gasvolume (without H_2O at 25°C)	[cm^3/g]	1049

The thermal decomposition behavior of most ionic liquids is still unknown due to the large number of combinations of substituted imidazoles, triazoles or tetrazoles as cation and various anions. But slow and rapid decomposition has already been investigated in several studies and mechanisms and kinetics are suggested [14, 15].

The decomposition mechanism of EILs depends on the nature of cation and anion and must be investigated in each case.

So Chowdhury et al. identify initiation and secondary reactions in the condensed phase for imidazole based ionic liquids in inert atmosphere, that lead to ignition and combustion under high heating rates and elevated temperatures [16].

Li et al. studied the behavior of 1-H-4-amino-1,2,4-triazolium nitrate, during thermal decomposition in inert environment driven by an infrared laser. They also focus on the initial decomposition reactions and subsequent reactions that lead to ring decomposition and ignition. Their results show that the most probable route to initiate the decomposition is through proton transfer from N1 site to the nitrate forming a neutral pair, nitric acid and amino-triazole. Subsequent reactions involve decomposition of the neutral pair and their interactions [17].

Litzinger et al. studied the initiation reactions of three classes of ionic liquids: imidazoles, 1,2,4-triazoles, and tetrazoles. They also investigated the decomposition behavior of 4-amino-1,2,4-triazolium nitrate in comparison to 1-methyl-4-amino-1,2,4-triazolium nitrate and suggested some reactions for a potential decomposition mechanism. Thus, proton transfer appears to be occurring even though the most readily transferred proton in the 1-position of the non-methylated species is not present in C1 N. In both cases nitric acid is formed, secondary reactions, such as the de-amination reactions involving NO^+, could lead to a removal of the amino-group form methyltriazole [18].

This paper focuses on the decomposition and especially combustion behavior of C1 N as an example of a typical EIL. Until now, no investigations were published on the burning behavior of EILs under inert, high-pressure conditions. So it must be reviewed if the results of possible decomposition reactions can be applied e.g. to the conditions in a rocket combustion chamber. In this study, burning velocities were measured as a function of pressure and initial temperature. From NIR-spectra temperature and species profiles were evaluated from the flame zone of C1 N energetic ionic liquid.

Experimental

To analyze the pure C1 N substance ^{1}H NMR and ^{13}C NMR were conducted on a 400 MHz Bruker AV-400 spectrometer in DMSO-d_6. Differential scanning calorimetry (DSC) was done by a TA Instruments Q 1000 using pierced aluminum pans. Scans were carried out on each sample at scan rates of 5 K/min under argon flux. Glass transition points were measured from the 2nd heating cycle after cooling to -90 °C. Reported values are onset temperatures. Thermogravimetric analysis (TGA) was done by a TA Instruments Q500 apparatus with a scan rate of 10 K/min under nitrogen flux. Reported values are the central points, according to DIN EN ISO 11358. Infrared spectroscopy was done on a Nicolet SX 5 spectrometer. Impact sensitivity and friction sensitivity tests were performed according to NATO STANAG 4487 and NATO STANAG 4489 procedures with the BAM-Impact sensitivity tester and the BAM-Friction sensitivity tester made by the former company Julius Peter (Berlin). Synthesis of C1 N was performed according to our published route [19] and purity of the C1 N was above 99.8% (IC and NMR). For all calorimetric measurements, an IKA C 2000 system was used. The calorimetric bomb was filled in each case with 5 mL water (HPLC purity) and after each run, the combustion products were examined for unburned carbon. The combustion experiment was repeated four times and nitric acid formation was determined by measuring the nitrate content in the water after each run. Reported values are the average of four measurements. Performance data were calculated with ICT Code [20], impulses are calculated with frozen equilibrium at a chamber pressure of 7 MPa and an expansion pressure of 0.1 MPa.

The burning behavior was investigated by using a high-speed color camera (MotionPro® X3 by Redlake) with a frame rate of 100 fps. The burning velocity or better-called progression rate was analyzed from the movies as described in [21]. In parallel, a series of emission spectra was captured by an UV/Vis/NIR spectrometer (Zeiss MCS 611 PGS-NIR 2.2) with an integration time of 50 ms per spectrum, at least for the samples tested under room temperature. The field of view of the spectrograph was limited with a horizontal slit aperture to achieve a local resolution of about 2 mm. The slit was positioned 40 mm above the test tube bottom. The spectra series were analyzed by the ICT-BaM software [22] using a modified method

described below to determine emission temperature and path length signals from various species. By multiplication of the time scale with the individual progression rate the time history was converted to the length scale in direction of the flame length. This is possible because the sample burns top down with a constant progression rate (see below).

The combustion tests were performed inside the ICT window bomb using nitrogen and argon as pressurizing gas up to 13 MPa. Therefore, C1 N was filled into test tubes of 70 mm length and an inner diameter of 6.7 mm. To ignite the samples, a melting wire enhanced by some milligram of a booster charge was placed close above the liquid surface. To realize different initial temperatures, the test tube was implemented into a cylindrical aluminum block (diameter 40 mm) using its heat capacity as a so-called recuperative cooler/heater. The block had a vertical slit of 5 mm width allowing the measurement of the progression rate. The samples were tempered inside the block to an adequate temperature. With thermocouples, the temperature of the EIL was controlled during tempering. Using a calibration procedure, it was determined how long it took to achieve the target temperature.

Results

Thermodynamic Calculations

The thermodynamic equilibrium composition of reaction products and the adiabatic temperature of C1 N as a function of pressure were calculated by ICT Thermodynamic Code [20] using the measured heat of formation of +33 kJ/mol as explained above [19]. The results are summarized in the diagram of Figure 2. Main products are nitrogen, hydrogen and carbon monoxide. With increasing pressure, the amount of hydrogen decreases slightly in balance with a minor increase of methane and water obeying the principle of Le Chatelier. This might also be the reason of the growth of the adiabatic temperature from 1600 K to 1680 K in the pressure range from 1 to 15 MPa.

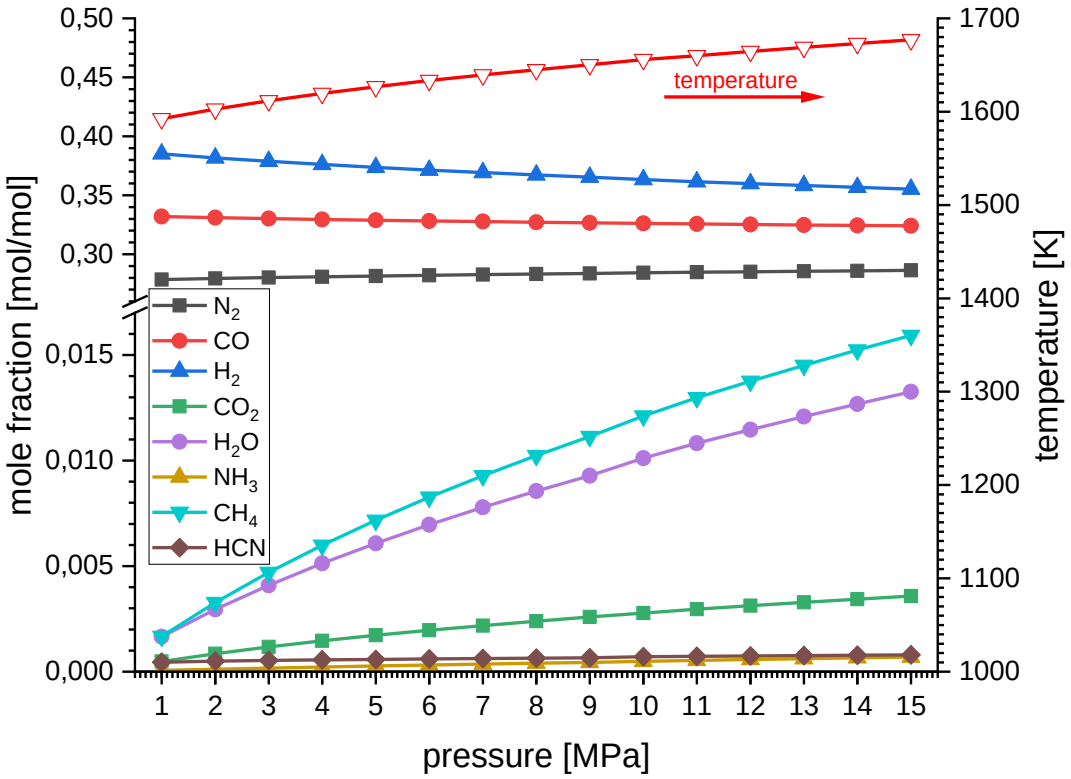

Figure 2 Equilibrium concentration and adiabatic temperature of AMTN combustion as function of pressure calculated with ICT-thermodynamic-code.

Thermoanalysis

Due to the negligible vapor pressure of ionic liquids, C1 N can be investigated with thermoanalytical methods as TG, DSC, EGA etc. with various heating rates HR.

The thermogravimetric mass loss is shown in Figure 3 performed with four different heating rates between 2 and 10 K/min. Depending on the heating rate, C1 N starts decomposition between 465 K (HR 2 K/min) and 480 K (HR 10 K/min). At 540 K, it is completely decomposed without any residue. Even when the curves look smooth, the decomposition and gasification process seem to be a complex mechanism as depicted in Figure 4 showing exemplary the differentiation of the TG-curve with HR 2 including various maxima and inflection points. A qualitative analysis with four fitted Gaussian curves indicates at least four different main reaction steps during the gasification. The half-width of the Gaussian curves decreases with increasing peak temperature of the reaction steps. The last step at about 530 K is a sharp peak only a few Kelvin in width.

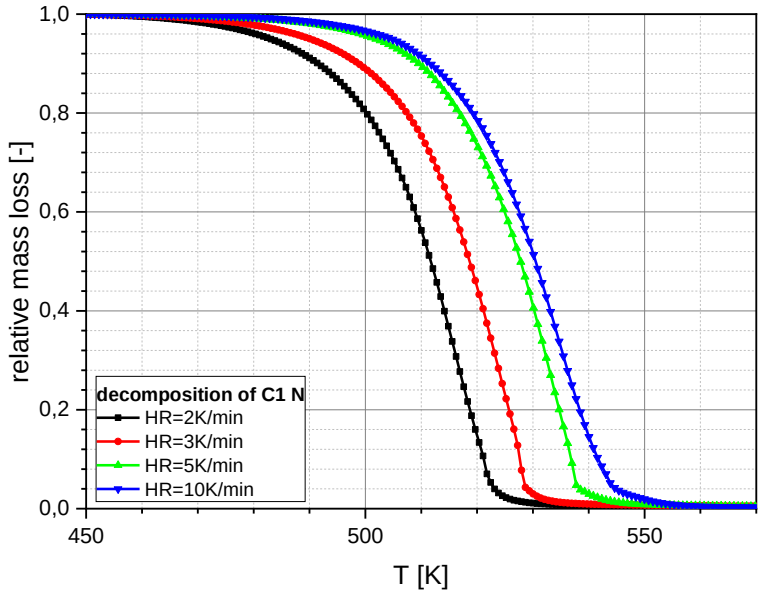

Figure 3 Thermogravimetric decomposition of C1 N at four different heating rates HR.

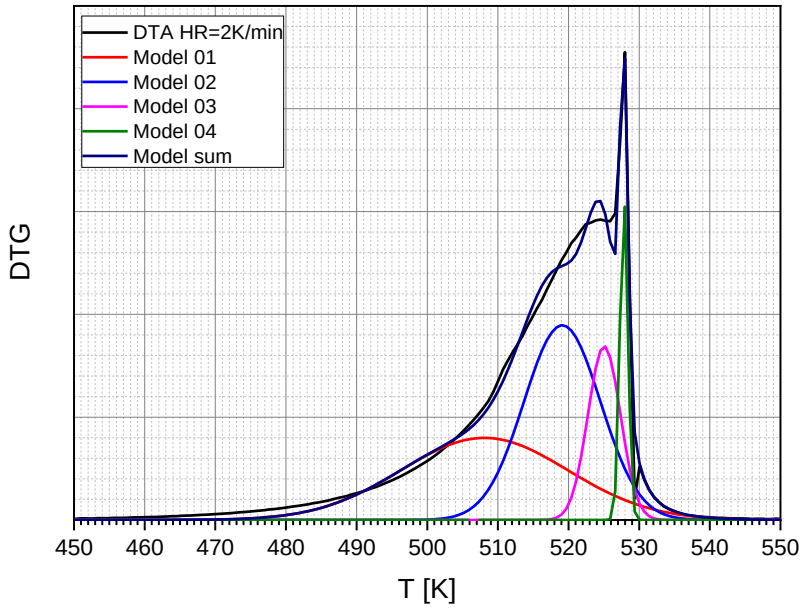

Figure 4 Differential thermogravimetric mass loss curves of C1 N and potential reaction steps modelled with Gaussian curves.

Corresponding investigations with differential scanning calorimetry (DSC) are presented in Figure 5 with four heating rates from 1 to 5 K/min. A comparison with the differential mass loss (Figure 4) almost shows the same curve shapes indicating that all reaction steps are exothermic and that the last step with the sharp peak is associated with a large and nearly spontaneous heat release.

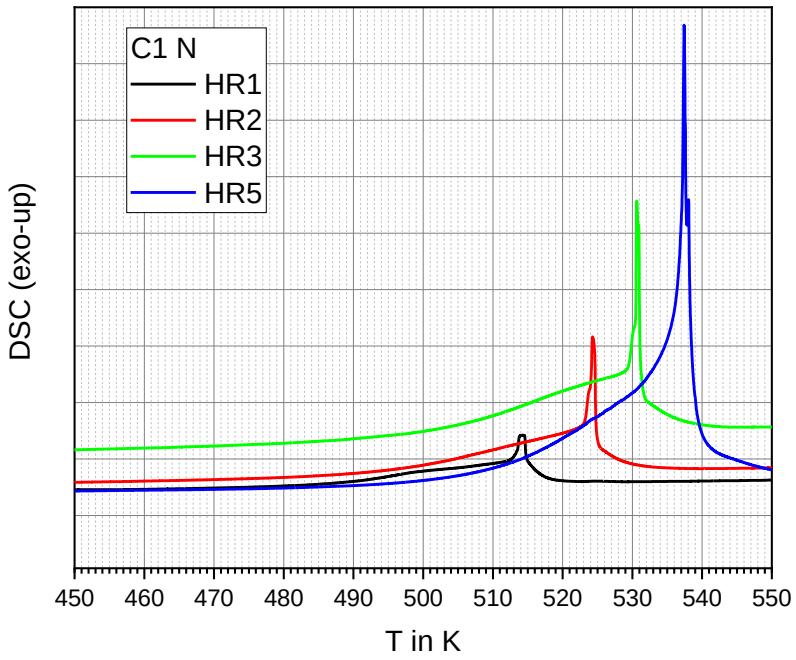

Figure 5 DSC curves of C1 N decomposition for four heating rates.

Evolved gas analysis (EGA) with FTIR in a heated pyrolysis cell with corresponding heating rates are not finally evaluated but first scans result in gaseous products at 540 K of nitrous oxide N_2O, carbon monoxide CO, water H_2O, hydrogen cyanide HCN and traces of ammonia NH_3. Carbon dioxide CO_2 could be detected too, but this also might be an atmospheric impurity.

Burning Behavior

Due to the low vapor pressure of energetic ionic liquids, a different burning mechanism and pressure dependency can be expected as it is found for other liquid propellants as nitromethane or isopropyl nitrate [23].

Pressure Deflagration Limits

The investigations of pure C1 N inside the window bomb under inert atmosphere and at various initial temperatures result in an unexpectedly high pressure deflagration limit (PDL) of at least 10 MPa, which is significantly higher than it is found for nitromethane. For most nitromethane-like energetic materials, the PDL decreases

with increasing initial temperature. But C1 N does not completely follow this trend. For 0 °C, PDL is 13 MPa, at room temperature (about 20 °C) and at 70 °C the PDL was determined to 10 MPa, but, at 40 °C, PDL is 12 MPa and thus significantly higher than at room temperature.

Burning Velocities as a Function of Pressure and Initial Temperature

In case of ignition, all samples burnt in a smooth way with a strictly linear progression rate (see Figure 6a). On the other hand, the combustion often suddenly stopped after 30 to 60 mm, leaving a rest of unburnt sample. The linear progression allowed determination of comparable burning velocities or better-called progression rates as a function of pressure and initial temperature. Figure 7 shows the results. In general, the values have a good reproducibility with a standard deviation of about 0.2 mm/s and do not differ significantly with pressure. To exclude a potential post reaction of the flame gases with the nitrogen, which is used as standard pressurizing gas, some tests were performed under argon resulting in the same progression rates in both atmospheres.

Most values spread between 6 and 7 mm/s and no influence of pressure was observed, even for initial temperatures between room temperature (RT) and 70 °C. Only the single values that could be measured at 13 MPa for an initial temperature of 0 °C are about 1.5 mm/s faster. For energetic materials, it is almost unusual that progression rates measured at lower initial temperature are faster than for higher temperatures. This phenomenon shall be clarified in future investigations.

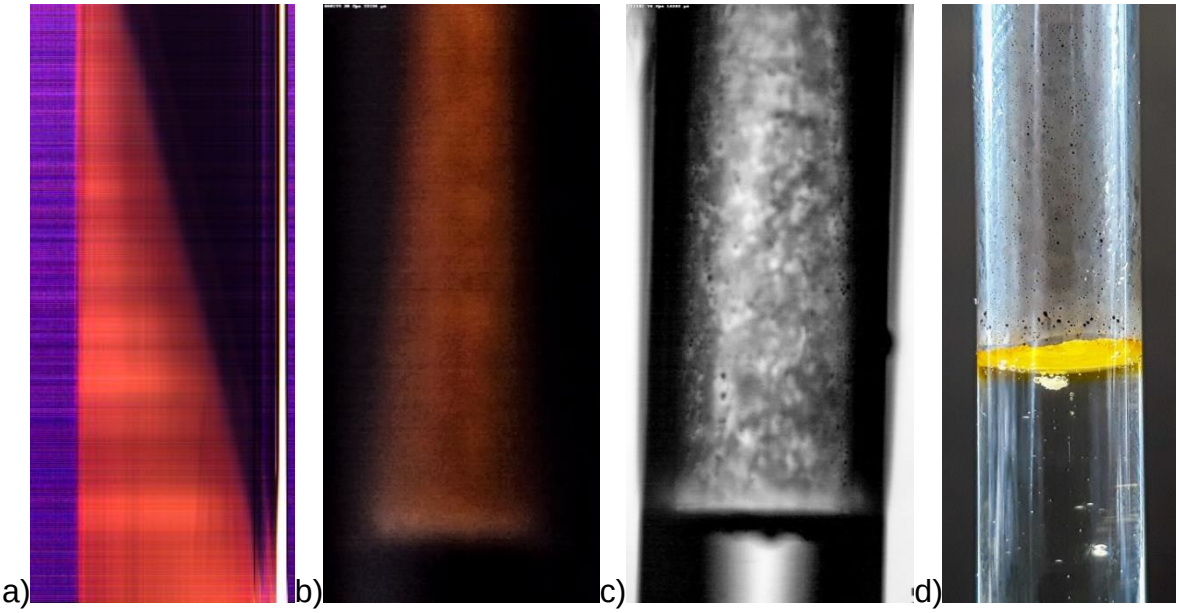

Figure 6 Burning of C1 N: a) linear progression, b) flame emission (amplified by image processing), c) burning observed with transmitted light, d) residue from extinguished sample.

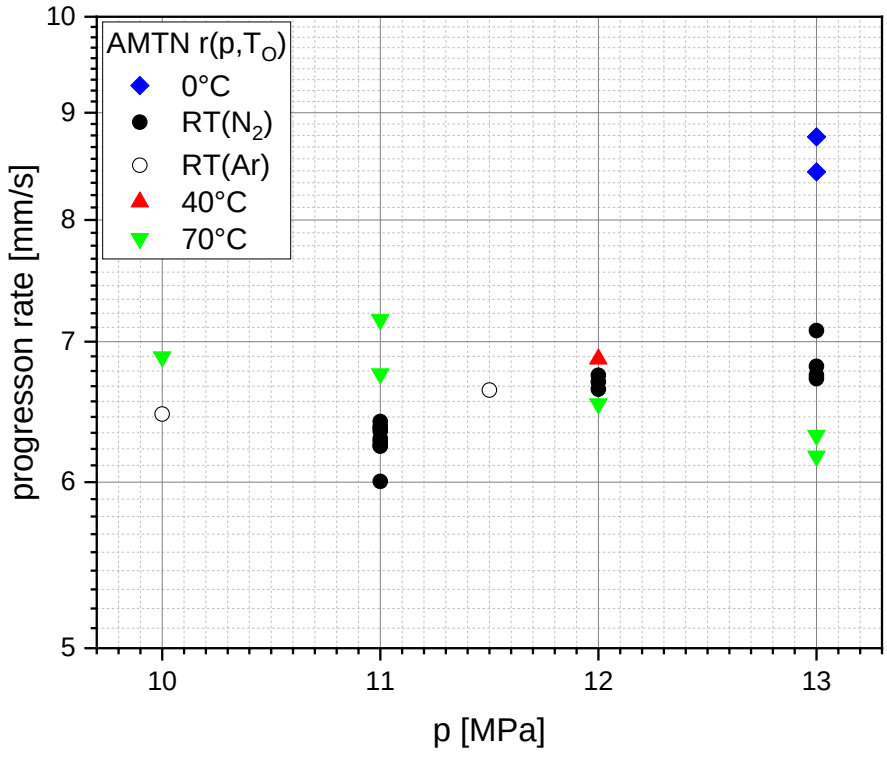

Figure 7 Progression rates from C1 N as function of pressure and initial temperature.

Visual Observations

The visual burning behavior does not differ significantly with pressure and initial temperature. The flame zone is nearly invisible, but by amplifying the video frames using picture processing a long, orange to red flame can be visualized (Figure 6b). The visible flame shape is nearly cylindrical or conic with more than 30 mm in length, independent of pressurizing gas, pressure and initial temperature. Close to the burning surface, a brighter nearly white flame layer of about 1 mm thickness can be observed in Figure 6b. Supplemental movies, taken with transmitted light, show an additional dark phase below the white flame layer located at the interface between condensed and gaseous phase. The high-speed movies also showed that this dark layer seems to swim on the EILs surface and did not change its shape during the progression. It could be identified as solid or at least gelatinous (Figure 6c). If a sample extinguishes, before it completely burnt down, this phase occurred in a yellow color (Figure 6d) for a short moment. When the burning finished, it starts to resolve in the remaining EIL after some time and got more and more gelatinous.

These observations confirm that the combustion or decomposition reaction of C1N is via a solid (possibly 1,2,4-triazole). This may lead to a first approach for a better understanding of the described burning behavior and shall be investigated in future work.

Emission Spectroscopy

Figure 8 shows a typical NIR-spectra series measured when a C1 N flame progresses through the field of view of the emission spectrometer.

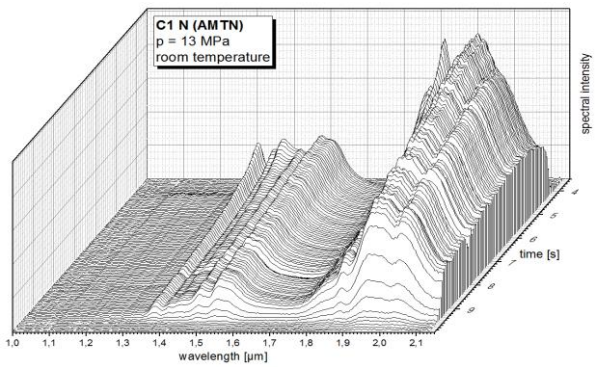

Figure 8 Typical series of spectra of the C1 N flame at room temperature and 13 MPa

Independent from the pressure level and the kind of pressurizing gas, the spectra have the same characteristics. Figure 9 shows the NIR-spectra between 1 and 2.15 µm taken at 12 MPa (thin lines) in comparison with a spectrum taken from an atmospheric C1 N pool fire in air, which solely shows water bands. Below 1 µm nearly no intensity was detected. The measured NIR emission spectra are typical for nitrogen rich organic energetic materials. Additionally, it was tried to assign the bands of the pressurized combustion of C1 N [24]. Beside the water bands, the spectra from the pressurized flame exhibit strong bands allocated to primary and secondary amines close to 1.56 µm and 2.03 µm and primary and secondary amides at 1.47 µm and 1.96 µm. These bands are unusual for nitrogen rich energetic materials like rocket and gun propellants or pure substances as nitro-amines burning under comparable conditions and are characteristic for the high-pressure combustion of azolium nitrates.

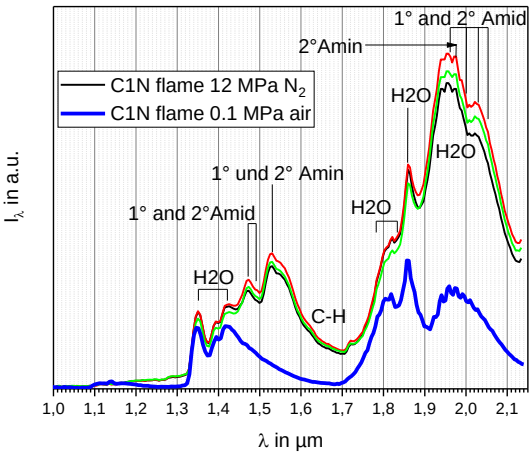

Figure 9 Exemplary NIR-spectra with spectral species allocation taken from the C1 N flame at 12 MPa in comparison with the emission of water taken from a C1 N flame in air.

Spectra Evaluation

The series of emission spectra were evaluated with the ICT-BaM software. This code is able to calculate theoretical spectra of grey and soot continuum emission and of most (N)IR emitting gas molecules (e.g. H_2O, CO, CO_2, NO, HCl …) as a function of species concentration (as concentration path length), temperature and pressure. To analyze measured spectra series, the code uses a least squares fit of calculated spectra to each measured one using temperature and concentration path length as parameters. The classical method for evaluating NIR spectra of energetic materials in

the range 1 to 2 µm is using a model, which combines grey body with water band emission. This method fails in the case of C1 N flame spectra due to the amine and amide emission overlapping the water bands. So additionally two Gaussian curves were introduced with central wavelengths at 1.56 µm (1° and 2° Amines) and 1.96 µm (1° and 2° Amides) and fixed line width of 0.045 µm and 0.035 µm. The amplitudes were used as further fit parameter representing a value proportional to the concentration path length of substances. Figure 10 compares fit curves to an exemplary C1 N spectrum (dots) using the method of grey emission with water bands (thin blue line[1]) and with two Gaussian curves (fat red line). The new method fits much better with significantly low χ^2 values. Therefore, it was assumed that also the achieved temperature and concentration values should be much more reasonable. Since the path length through the flame is not known but can be assumed as equal for all gaseous species the results from each spectra series can be compared as the expression of standardized intensity (I/I_0).

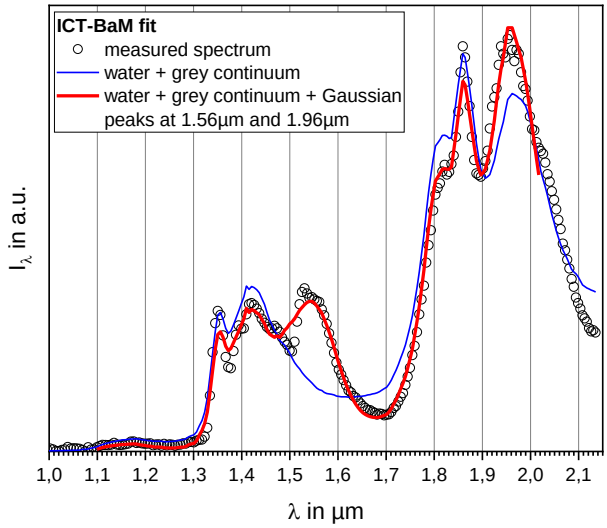

Figure 10 Exemplary spectrum analyzed with different ICT-BaM methods

First results of intensity profiles are presented determined by the integration of each spectrum of a series from 0.3 to 2.15 µm. In Figure 11, four of such profiles are plotted. Two received at 11 MPa (fat blue line), the others at 13 MPa (thin red line). As the burning surface of the EIL is a horizontal plain (comp. Figure 6) the signal

[1] For color information see digital text version

should be a step function at this position. The measured intensities increase over a distance of about 2 mm giving a realistic idea of the spatial resolution of the spectral data. The surface position x = 0 mm was assumed to be at the 50% value of the intensity increase. The profiles indicate a reasonable reproducibility and a minor increase of intensity with increasing pressure. Signal intensity starts about 5 mm below the surface position. Water band spectra from this zone consist in overlapping emission and absorption signals, which could not be analyzed according to water band temperature, but continuum radiation and the Gaussian curves could be evaluated. After the intensity passed a maximum, it is decreasing nearly linearly over about 30 to 35 mm. Presumably, this is a consequence of the decreasing width of the conical flame shape. At least, the signal interrupts. Due to the slit position, this part does not match with the flame tip but with the extinguishment of the flame close to the bottom of the test tube. Therefore, this part was not included in the analysis of water band temperature and species.

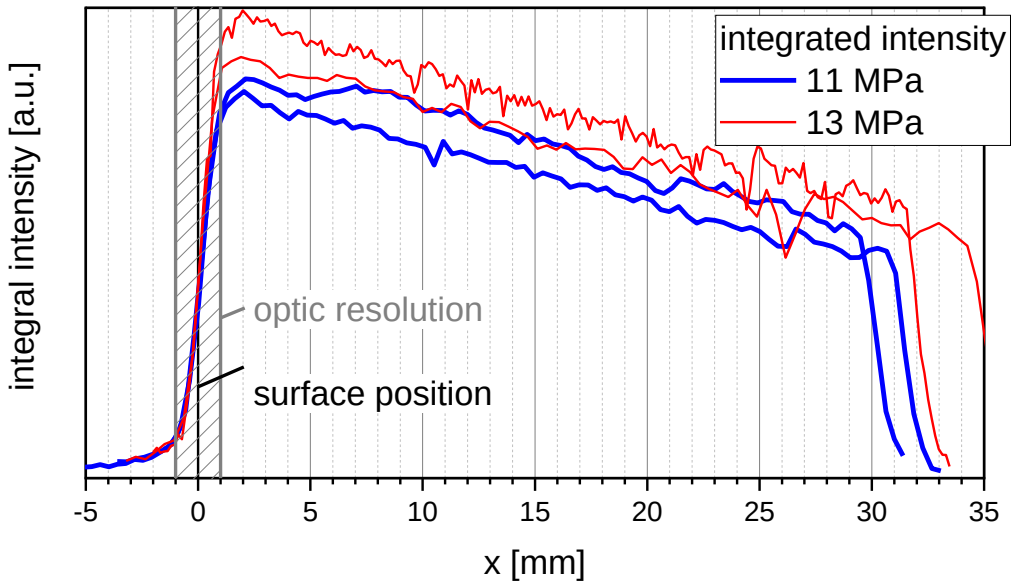

Figure 11 Profiles of integrated intensity received from spectra series of C1 N flames at 11 MPa and 13 MPa

Temperature Profiles

The temperature profiles of continuum emission spectra (thin lines) and the water bands (thick lines) of the same spectra series of C1 N flames at 11 MPa (dark) and 13 MPa (light) are plotted in Figure 12. Mainly, continuum radiation is emitted from

solid surfaces caused by the heated glass walls of the used test tube and below the burning surface. The water band temperature is associated to the flame. The flame temperature profiles start with about 1600 K close to the surface and continuously increase up to 2000 K or even higher over a range of about 20 mm, before reaching a plateau. The surface temperatures seem to be independent from the pressure. However, at 13 MPa the temperature in the flame zone rises to higher values than at 11 MPa. When evaluating the water band spectra usually the temperature information is included within the shape of the bands and the intensity ratio of different bands. Due to the modified method of ICT-BaM evaluation, the temperature can be derived from the intensity of only the two main water peaks at 1.35 µm and 1.85 µm. In consequence, the accuracy of temperature determination is worse. Usually it deviates of about 5%, but in this case, a value of about 20% shall be presumed. This but also the above discussed difficulty to determine the heat of formation might explain flame temperatures higher than the adiabatic temperature calculated with ICT Thermodynamic Code (comp. Figure 2). However, these considerations will not affect the trend of the increasing flame temperatures.

Close to the surface, the continuum temperature features in a maximum close to 700 K. But the gas temperature at this position is low. This maximum of the glass wall temperature can only be explained by exothermic reactions below the burning surface of the EIL. This is also in agreement with the DSC studies (comp. Figure 5).

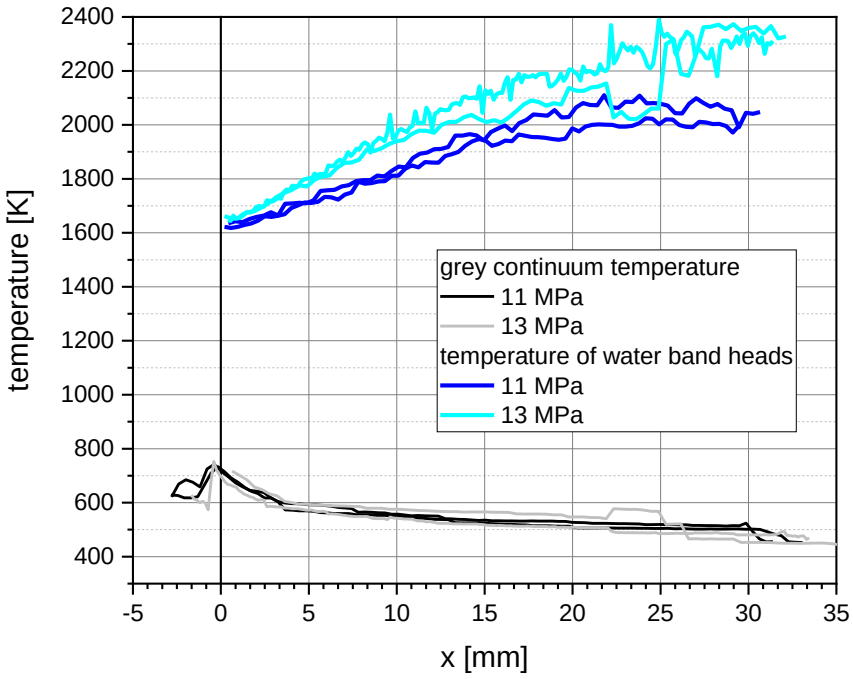

Figure 12 Temperature profiles of continuum emission and the water bands of C1 N flames at 11 MPa and 13 MPa

Exemplary profiles of some species in the flame zone of C1 N at 11 MPa (dotted line) are plotted in Figure 13 normalized between 0 and 1. Additionally, the integrated intensity is shown as grey dotted line. The corresponding temperature profiles received from continuum and water band analysis are given as well (fat lines, right ordinate). Due to the discussed lack of knowledge about the flame tip, the position scale is cut at x = 30 mm. At the surface, a significant signal from emitting water is seen increasing for about 1 mm to a maximum and completely decreasing along the flame. This indicates that water is produced during the decomposition of the EIL at the surface reaction zone, but it is also formed in the gas phase by the reaction of primary gaseous decomposition products. The peaks of the Gaussian curves at 1.56 µm and 1.96 µm, which are related to primary and secondary amines and amides can be identified also below the surface, but it is not sure if this is caused by scattering or reflection effects or indicates an actual reaction. The bands from above the surface at 1.56 µm related to amines increase nearly as fast as the water bands. However, the position of the maximum is up to 5 mm higher and the slope afterwards is much less than for water bands and nearly parallel to the slope of the integrated intensity. This indicates a more important effect of path length than a concentration decrease.

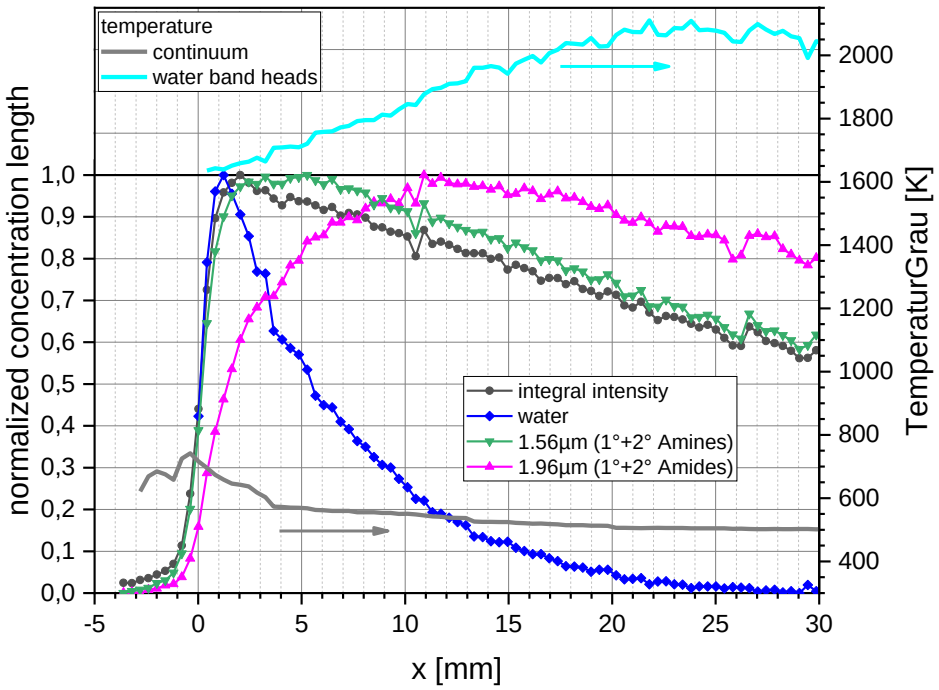

Figure 13 Profiles of determined normalized concentration length and temperatures from a C1 N flame at 11 MPa.

Recently an evaluation of the emission spectra was started using chemometric tools. First results indicate a good agreement between this physical evaluation with ICT-BaM and the chemometric multivariate curve resolution (MCR). The MCR results revealed a good agreement between the estimated and measured spectra and the estimated concentration profiles. This study will be published soon after completion.

Conclusion

4-Amino-1-methyl-1,2,4-triazoliumnitrat (C1 N or AMTN) is an energetic ionic liquid with moderate performance properties, but a characteristic substance for a wide class of this kind of energetic materials [19], which can be synthesized in technical amounts. Therefore, it is used in this study as model substance to investigate the decomposition, gasification and combustion behavior under inert conditions. At atmospheric pressure, the EIL decomposes completely at around 500 K to gaseous species in a reaction mechanism of at least four main steps. By FTIR analysis N_2O, CO, H_2O, HCN and NH_3 were identified in the gas phase at 540 K.

At inert high-pressure conditions, pure C1 N could only be ignited at more than 10 MPa. Then it burns with a constant progression rate forming a long flame featuring in temperatures close to the adiabatic temperature of about 1700 K increasing slowly with the flame axis and pressure. At the condensed-gaseous interface, a hot solid or gelatinous reaction zone of about 1 mm thickness was found. Burning rates between 6 to 9 mm/s were measured as a function of pressure and initial temperature without detecting a significant influence of these conditions. A pressure exponent close to zero appears to be significant for this class of EILs [19]. Supported by the visual and spectral investigations this indicates that an exothermic gasification process is proceeded at or maybe inside the solid burning surface producing gaseous species, which will further react exothermically, but with a relative slow reaction rate. This is indicated by a significant temperature increase along a distance of about 20 mm above the burning surface. As known from solid propellant combustion investigations only temperature gradients over a distance of less than hundred micrometers above the burning surface are responsible for the pressure dependence of such materials. For the investigated EIL, this distance is much longer and may explain the detected low pressure dependence of the material.

References

[1] (a) T. Welton, *Chem. Rev.* 1999, 99, 2071-2083. (b) P. Wasserscheid, W. Keim, *Angew. Chem. Int. Ed.* 2000, 39, 3772-3789.

[2] P. Wasserscheid, T. Welton*, Ionic Liquids in synthesis*, Wiley-VCH, 2002.

[3] (a) H. Shobukawa, H. Tokuda, A. B. H. Susan, M. Watanabe, *Electrochim. Acta* 2005, 50, 3872-3877. (b) H. Shobukawa, H. Tokuda, S. Tabata, M. Watanabe, *Electrochim. Acta* 2004, 50, 1-5. (c) S. Seki, Y. Kobayashi, H. Miyashiro, Y. Ohno, *Chem. Commun.* 2006, 544-545.

[4] D. Kuang, S. Uchida, R. Humphry-Baker, S. M. Zakeeruddin, M. Grätzel, *Angew. Chem.* 2008, 120, 1949-1953.

[5] (a) D. J. Tempel, P. B. Henderson, J. R. Brzozowski, R.M. Pearlstein, D. Garg, US Pat. *20060060818*, 2006. (b) D. J. Tempel, P. B. Henderson, J. R. Brzozowski, US Pat. *20060060817*, 2006.

[6] (a) C. Ye, W. Liu, Y. Chen, L. Yu, Chem. Commun. 2001, 2244-2245. (b) X. Liu, F. Zhou, Y. Liang, W. Liu, *Wear* 2006, 261, 1174-1179. (c) T. Predel, E. Schlücker, P. Wasserscheid, D. Gerhard, W. Artl, *Chem. Eng. Technol.* 2007, 30, 1475-1480.

[7] M. E. V. Valkenburg, R. L. Vaughn, M. Williams, J. S. Wilkes, *Thermochim. Acta* 2005, 425, 181-188.

[8] S. Gabriel, J. Weiner, *Ber*. 1888, 21, (2), 2669-2679.

[9] (a) P. Walden, *Chem. Zentralbl*. 1914, (I), 1800. (b) N. V. Plechkova, K. R. Seddon, *Chem. Soc. Rev.* 2008, 37, 123-150.

[10] (a) H. Xue, J. M. Shreeve, Adv. Mater. 2005, 17, 2142-2416. (b) H. Xue, Y. Gao, B. Twamley, J. M. Shreeve, Chem. Mater., 2005, 17, (1), 191-198. (c) Y. Gao, H. Gao, C. Piekarski, J. M. Shreeve, Eur. J. Inorg. Chem. 2007, 31, 4965-4972. (d) R. Wang, R.; H. Gao, C. Ye, B. Twamley, J. M. Shreeve, Inorg. Chem. 2007, 46, 932-938.

[11] (a) G. Drake, T. Hawkins, "Research in Energetic Ionic Liquids", Report AFRL-PR-ED-VG-2002-232, 2002. (b) G. Drake, T. Hawkins, K. Tollison, L. Hall, "1-Alkyl-4-Amino-1,2,4-Triazolium Salts, New Families of Ionic Liquids", Report AFRL-PR-ED-TP-2003-307, 2003.

[12] (a) Diallo, A. O.; Len, C.; Morgan, A. B.; Marlair, G. Revisiting Physico-Chemical Hazards of Ionic Liquids. *Sep. Purif. Technol.* 2012, *97 (ILSEPT2011 Special Issue)*, S. 228–234.

[13] Xue, H.; Arritt, S. W.; Twamley, B.; Shreeve, J. M. Energetic Salts from N-Aminoazoles. Inorg. Chem. 2004, 43 (25), S. 7972–7977

[14] M. C. Kroon, W. Buijs, C. J. Peters, G.-J. Witkamp, Quantum chemical aided prediction of the thermal decomposition mechanisms and temperatures of ionic liquids, Thermochimica Acta 465 (2007) 40–47

[15] A. Chowdhurya, S. T. Thynella, P. Lin, Confined rapid thermolysis/FTIR/ToF studies of tetrazolium-based energetic ionic liquids, Thermochimica Acta 485 (2009) 1–13

[16] A. Chowdhury, S. T. Thynel, Confined rapid thermolysis/FTIR/ToF studies of imidazolium-based ionic liquids, Thermochimica Acta 443 (2006) 159–172

[17] J. Li, T. A. Litzinger, Thermal decomposition of 4-amino-1,2,4-triazolium nitrate under infrared laser heating, Thermochimica Acta 454 (2007) 116–127

[18] T. A. Litzinger, S. T. Thynell, Condensed-phase Reactions of Energetic Ionic Liquids under Different Ignition Stimuli, Final Performnance Report, GRANT NUMBER: F49620-03-1-0211, (2007), Pennsylvania State University, 110 Technology Center, University Park

[19] U. Schaller, Synthese und Charakterisierung von energetischen ionischen Liquiden auf Basis von 4-Amino-1,2,4-triazol - Stuttgart: Fraunhofer Verlag, [2016]. - (Wissenschaftliche Schriftenreihe des Fraunhofer ICT ; Band 67) Universität Stuttgart, Dissertation, 2015.

[20] S. Kelzenberg, P. Kempa, S. Wurster, M. Herrmann, T. Fischer, New Version Of The ICT-Thermodynamic Code, 45th International Annual Conference of ICT, June 24 - 27, 2014, Karlsruhe, Germany Pfinztal: Fraunhofer ICT, 2014 pp. 95.1-95.9.

[21] V. Weiser, H. Ebeling, M. Weindel, W. Eckl, T. Klahn, Non-intrusive burning rate measurement under pressure by evaluation of video data; 35th International Annual Conference of ICT, June 29-July 2, 2004, Karlsruhe, pp. 158-(1-6)

[22] V. Weiser, N. Eisenreich, Fast Emission Spectroscopy for a Better Understanding of Pyrotechnic Combustion Behavior, Propellants, Explosives, Pyrotechnics, 30(1), 2005, pp. 67–78.

[23] S. Kelzenberg, N. Eisenreich, W. Eckl, V. Weiser, Modelling Nitromethane Combustion; Propellants, Explosives, Pyrotechnics 24; 189-194 (1999)

[24] J. Workman Jr., L. Weyer; Practical Guide and Spectral Atlas for Interpretive Near-Infrared Spectroscopy, Second Edition; CRC Press; Taylor & Francis Group (2012)